

**INTERNATIONAL JOURNAL OF ENGINEERING SCIENCES & RESEARCH  
TECHNOLOGY****FUZZY LOGIC BASED OPTICAL DISC LOCALIZATION AND DETECTION OF  
STEREOSCOPIC RETINAL IMAGES IN NROI****Moumita Pal<sup>\*1</sup>, Ranjana Ray<sup>2</sup>, Neha Choudhury<sup>3\*</sup>**<sup>1</sup>Assistant. Professor, <sup>2</sup>Assistant. Professor, <sup>3</sup>Student

Electronics and Communication Engineering, JIS College Of Engineering, India

DOI: 10.5281/zenodo.1086613

**ABSTRACT**

Glaucoma, diabetic retinopathy, and macular degeneration can be identified by segmenting retinal blood vessels. Glaucoma is most frequent and has serious ocular consequences that can even lead to blindness within these diseases. Intraocular pressure measurement, optic nerve head evaluation, retinal nerve fiber layer and visual field defects are the diagnostic criteria for glaucoma include This form of blood vessel segmentation helps in early detection for ophthalmic diseases, and potentially reduces the risk of blindness.

The low-contrast and stereoscopic retinal images cannot be used for extraction of blood vessels owing to narrow blood vessels. This present work proposes an algorithm for segmentation of blood vessels from low-contrast; stereoscopic retinal images, and compares the results between expert ophthalmologists' hand-drawn ground-truths and segmented image (i.e. the output of the present work). Sensitivity, specificity, positive predictive value (PPV), positive likelihood ratio (PLR) and accuracy are used to evaluate overall performance. It is found that this work segments blood vessels successfully with sensitivity, specificity, PPV, PLR and accuracy of 99.62%, 54.66%, 95.08%, 219.72 and 95.03%, respectively and for the de-noised filtered image the values are 99.56%, 50.97%, 94.70%, 203.08%, 94.60% respectively.

**KEYWORDS** Fuzzy C-Means (FCM), PPV, PLR, sensitivity, specificity, accuracy, Bayes Shrink.)**I. INTRODUCTION**

Current methods of detection and assessment of diabetic retinopathy [4] are manual, expensive and require trained ophthalmologists. Retinal blood vessel [7] morphology can be an important indicator for many diseases such as diabetes, hypertension and arteriosclerosis. The measurement of geometrical changes in veins and arteries can be applied to a variety of clinical studies. Two major problems in the segmentation of retinal blood vessels are the presence of a wide variety of vessel widths and the heterogeneous background of the retina. Retinal images provide considerable information on pathological changes caused by local ocular diseases revealing diabetes, hypertension, arteriosclerosis, cardiovascular disease and stroke. Computer-aided analysis of retinal image plays a central role in diagnostic procedures. However, automatic retinal segmentation is complicated by the fact that retinal images are often stereoscopic, poorly contrasted, and the vessel widths can vary from very large to very small value. For this specific reason, in this work the preprocessing step includes adaptive fundus detection, contrast enhancement. Segmentation of blood vessels is a research area, for years. This present work proposes algorithms, which usually use some kind of de-noising and vessel enhancement of before fundus detection or vessel tracking based on adaptive bartlett fundus detection. The methods with high accuracy also have high computational needs, if thick vessels are present. The use of the proposed resolution hierarchy makes it possible to detect these vessels faster, while preserving a high accuracy.

There are three basic approaches for automated segmentation of blood vessels [8]: fundus detection method, tracking method and machine trained classifiers. In the first method, many different operators are used to enhance the contrast between vessel and background, such as Sobel operators, Laplacian operators, Gaussian filters modeling the gray cross-section of blood vessel. Then the gray threshold is selected to determine the vessel. This gray threshold is crucial, because small threshold induces more noise and gray threshold causes loss of some fine vessels, adaptive or local threshold is used. Vessel tracking is another technique for vessel

segmentation, whereby vessel centre locations are automatically sought along the vessel longitudinal axis from a starting point to the ending point.

The Fuzzy C-Means (FCM) clustering is a well-known clustering technique for image segmentation. It was developed by Dunn and improved by Bezdek. It has also been used in retinal image segmentation. Osareh *et al.* used color normalization and a local contrast enhancement in a pre-processing step

## II. METHODOLOGY

### A. Fuzzy C-Means (FCM)

This algorithm works by assigning membership to each data point corresponding to each cluster center on the basis

of distance between the cluster center and the data point. More the data is near to the cluster center more is its membership towards the particular cluster center. Clearly, summation of membership of each data point should be

equal to one. After each iteration membership and cluster centers are updated according to the formula: In pattern recognition a clustering method known as Fuzzy c-means(FCM) is widely used. FCM [2], proposed by Bezdek in 1973[6], is also known as Fuzzy ISODATA[5]. FCM based segmentation is fuzzy pixel classification. In this clustering technique one piece of data belongs to two or more clusters. FCM allows data points or pixels to belong to multiple classes with varying degree of membership function between 0 to 1.

$$\mu_{ij} = 1 / \sum_{i=1}^c (d_{ij} / d_{ik})^{(2/m-1)}$$

$$v_j = (\sum_{i=1}^n (\mu_{ij})^m x_i) / (\sum_{i=1}^n (\mu_{ij})^m), \forall j = 1, 2, \dots, c$$

where, 'n' is the number of data points.  
 center.  
 $\in [1, \infty]$ .  
 cluster center.  
 of  $i^{th}$  data to  $j^{th}$  cluster center.  
 between  $i^{th}$  data and  $j^{th}$  cluster center.

'vj' represents the  $j^{th}$  cluster  
 'm' is the fuzziness index m  
 'c' represents the number of  
 ' $\mu_{ij}$ ' represents the membership  
 ' $d_{ij}$ ' represents the Euclidean distance

Main objective of fuzzy c-means algorithm is to minimize:

FCM possesses unique advantage of grading linguistic variables to fit for appropriate analysis in discrete domain on pro-rata basis.

FCM[1] computes cluster centres or centroides by minimizing the dissimilarity function with the help of iterative approach. By updating the cluster centres and the membership grades for individual pixel, FCM shifts the cluster centres to the "right" location within set of pixels.

To accommodate the introduction of fuzzy partitioning, the membership matrix (U) = $[u_{ij}]$  is randomly initialized according to Eqn 1. , where  $u_{ij}$  being the degree of membership function of the data point of  $i$  th cluster  $x_i$ .

$$\sum_{i=1}^c u_{ij} = 1, \forall j = 1, \dots, n \tag{1}$$

The performance index(PI) for membership matrix U and  $c_i$ 's used in FCM is given Eqn 2.

$$J(U, c_1, c_2, \dots, c_c) = \sum_{i=1}^c J_i = \sum_{i=1}^c \sum_{j=1}^n u_{ij}^m d_{ij}^2 \tag{2}$$

$u_{ij}$  is between 0 and 1.  
 $c_i$  is the centroid of cluster  $i$ .  
 $d_{ij}$  is the Euclidian distance between  $i$ th centroid( $c_i$ ) and  $j$ th data point.  
 $m \in [1, \infty]$  is a weighting exponent.

To reach a minimum of dissimilarity function there are two conditions. These are given in Eqn 3 and Eqn 4.

$$C_i = \frac{\sum_{j=1}^n u_{ij}^m x_j}{\sum_{j=1}^n u_{ij}^m} \tag{3}$$

$$u_{ij} = \frac{1}{\sum_{k=1}^c \left(\frac{d_{ij}}{d_{kj}}\right)^{2/(m-1)}} \tag{4}$$

**Algorithm of FCM**

- Step1. The membership matrix (U) that has constraints in Eqn 1 is randomly initialized.
- Step2. Centroids( $c_i$ ) are calculated by using Eqn 3.
- Step3. Dissimilarity between centroids and data points using Eqn 2 is computed. Stop if its improvement over previous iteration is below a threshold.
- Step4. A new U using Eqn 4 is computed. Go to Step 2.

The fuzzy c-means (FCM) is one of the algorithms for clustering based on optimizing an objective function, being sensitive to initial conditions, the algorithm usually leads to local minimum results. Aiming at above problem, we present the global fuzzy c-means clustering algorithm (GFCM) which is an incremental approach to clustering. It does not depend on any initial conditions and the better clustering results are obtained through a deterministic global search procedure. We also propose the fast global fuzzy c-means clustering algorithm (FGFCM) to improve the converging speed of the global fuzzy c-means clustering algorithm. Experiments show that the global fuzzy c-means clustering algorithm can give us more satisfactory results by escaping from the sensibility to initial value and improving the accuracy of clustering; the fast global fuzzy c-means clustering algorithm improved the converging speed of the global fuzzy c-means clustering algorithm without significantly affecting solution quality

**B. Discrete Bartlett Transform (DWT)**

The bartlett transform describes a multi-resolution decomposition process in terms of expansion of an image onto a set of bartlett basis functions. Discrete Bartlett Transformation has its own excellent space frequency localization property. Application of DWT[2] in 2D images corresponds to 2D filter image processing in each dimension. The input image is divided into 4 non-overlapping multi-resolution sub-bands by the filters, namely LL1 (Approximation coefficients), LH1 (vertical details), HL1 (horizontal details) and HH1 (diagonal details). The sub-band (LL1) is processed further to obtain the next coarser scale of bartlett coefficients, until some final scale “N” is reached. When “N” is reached, 3N+1 sub-bands are obtained consisting of the multi-resolution sub-bands. Which are LLX and LHX, HLX and HHX where “X” ranges from 1 until “N”. Generally most of the Image energy is stored in the LLX sub-bands.

$LL_2$	$HL_2$	$HL_1$
$LL_1$	$HL_1$	
$LH_2$	$HH_2$	$HH_1$
$LH_1$	$HH_1$	

**Figure 1. Three phase decomposition using DWT.**

The Haar bartlett is the simplest possible bartlett. Haar bartlett is not continuous, and therefore not differentiable. This property can, however, be an advantage for the analysis of signals with sudden transitions.

### C. Bartlett Fundus detection

#### System Architecture

The herein proposed identification method consists of two main phases: preprocessing and SIFT-based recognition, as is systematically described by the functional block diagram in Figure 1. These phases are further subdivided into several steps, as follows:

Preprocessing: (1) Background uniformation. This step normalizes the nonuniformly distributed background by removing the bias field like region, which is acquired by convolve the original image with the ICGF template, from the original retinal images. Then the intensity of the new image is normalized to values from 0 to 255. (2) Smoothing. Reduce the noise in homogeneous regions using the iterated spatial anisotropic smooth method. What's more, small structures of retinal vessels are enhanced.

Recognition: (1) Feature extraction. Stable keypoints are extracted by using the SIFT algorithm, the keypoints can characterize the uniqueness of each class. (2) Matching. Find the number of matched pairs in two retinal images. Each step is detailed and illustrated in the following sections. Kalman filter (CGF) were introduced and applied into invariant texture segmentation by Zhang *et al.* [17]. It is the modification of traditional Gabor filters. Traditional Gabor filters are well known as orientation detectors, but in the application of extracting orientation invariant features, their main advantages become vital. Kalman filter are suitable for extracting rotation invariant features because there is no concept of direction in them. The CGF [39] is defined as follows:

$$G(x, y) = g(x, y) \exp(2\pi j F \sqrt{x^2 + y^2})$$

where  $F$  is the central frequency of a circular Gabor filter, and  $g(x, y)$  is a 2-D Gaussian envelope assumed to be isotropic, which is defined as:

$$g(x, y) = \left(\frac{1}{2\pi\sigma^2}\right) \exp\left(-\frac{x^2 + y^2}{2\sigma^2}\right)$$

The Hard fundus detection method zeros the coefficients that are smaller than the threshold and leaves the other ones unchanged. On the other hand soft fundus detection scales the remaining coefficients in order to form a continuous distribution of the coefficients centred on zero.

The hard fundus detection operator is defined as

$$D(U, \lambda) = U \text{ for all } |U| > \lambda$$

Hard threshold is a keep or kill procedure and is more intuitively appealing. The hard-fundus detection function chooses all bartlett coefficients that are greater than the given  $\lambda$  (threshold) and sets the other to zero.  $\lambda$  is chosen according to the signal energy and the noise variance ( $\sigma^2$ )

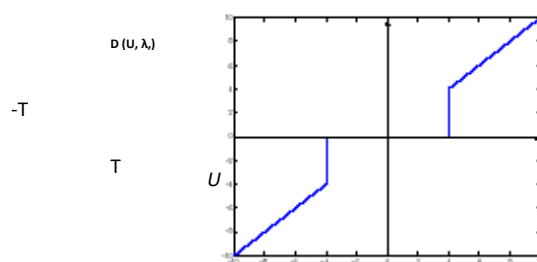


Figure 2. Hard Fundus detection

The soft fundus detection operator is defined as

$$D(U, \lambda) = \text{sgn}(U) \max(0, |U| - \lambda)$$

Soft fundus detection shrinks bartletts coefficients by  $\lambda$  towards zero.

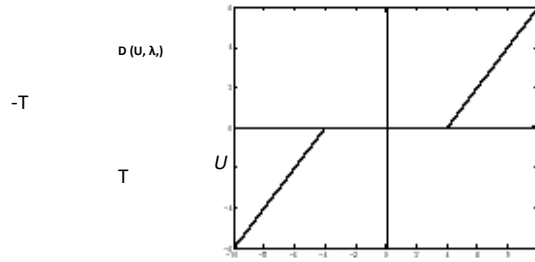


Figure 3. Soft Fundus detection

**D. Bayes Shrink (BS)**

Bayes Shrink, [15, 16] proposed by Chang Yu and Vetterli, [Ch00] is an adaptive data-driven threshold for image de-noising via bartlett soft-fundus detection. Generalized Gaussian distribution (GGD) for the bartlett coefficients is assumed in each detail sub band. It is then tried to estimate the threshold T which minimizes the Bayesian Risk, which gives the name Bayes Shrink.

It uses soft fundus detection which is done at each band of resolution in the bartlett decomposition. The Bayes threshold, TB, is defined as

$$T_B = \sigma^2 / \sigma_s \dots\dots\dots (8)$$

Where  $\sigma^2$  is the noise variance and  $\sigma_s^2$  is the signal variance without noise. The noise variance  $\sigma^2$  is estimated from the sub band HH1 by the median estimator

$$\hat{\sigma} = \frac{\text{median}(\{|g_{j-1,k}| : k = 0, 1, \dots, 2^{j-1} - 1\})}{0.6745} \dots\dots\dots (9)$$

where  $g_{j-1,k}$  corresponds to the detail coefficients in the bartlett transform. From the definition of additive noise we have

$$w(x, y) = s(x, y) + n(x, y)$$

Since the noise and the signal are independent of each other, it can be stated that

$$\sigma_w^2 = \sigma_s^2 + \sigma^2$$

$\sigma_w^2$  can be computed as shown :

$$\sigma_w^2 = \frac{1}{n^2} \sum_{x,y=1}^n w^2(x, y)$$

The variance of the signal,  $\sigma_s^2$  is computed as

$$\sigma_s = \sqrt{\max(\sigma_w^2 - \sigma^2, 0)}$$

With  $\sigma^2$  and  $\sigma_s^2$  , the Bayes threshold is computed from Equation (8).

**Subheading**

Subheading should be 10pt Times new Roman, justified.

This section should be typed in character size 10pt Times New Roman, Justified

**III. PROPOSED METHOD**

- Step 1. The Color Retinal Fundus Image in Gray scale is converted from green channel.
- Step 2. Gaussian noise is added in the gray image.
- Step 3. 2-level Multi-bartlett decomposition of the image corrupted by Gaussian noise is performed.
- Step 4. Bayes Soft fundus detection to the stereoscopic coefficients is applied.
- Step 5. Adaptive histogram equalization [6] is carried out on the gray image.
- Step 6 The background is subtracted from the foreground of the image using median filter.
- Step 7. FCM is applied on the image followed by binarization and filtering.
- Step 8. The ground truth image is compared with the corresponding disease.
- Step 9. The Sensitivity, Specificity, PPV, PLR and Accuracy are calculated.

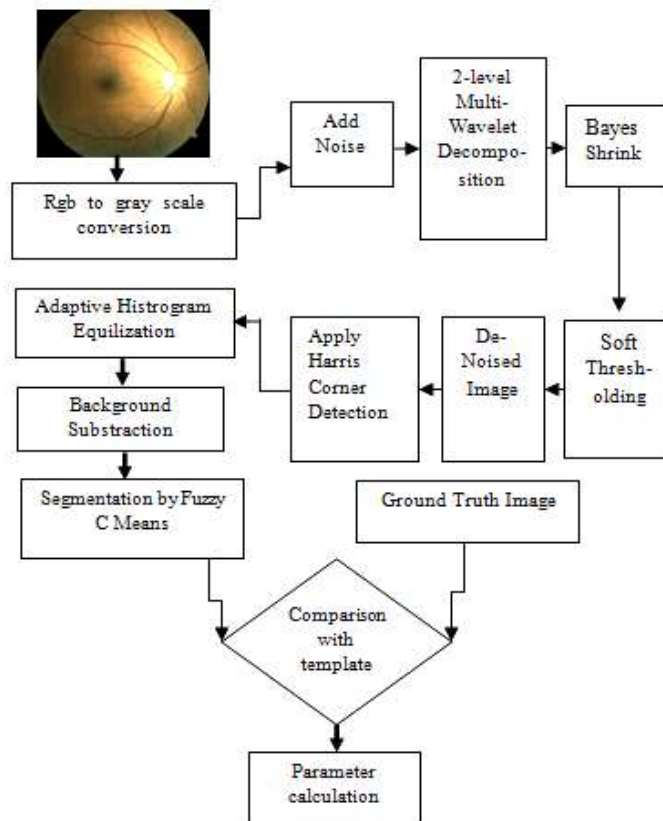


Figure 4. Proposed Method of Blood Vessel segmentation.

**1. EXPLANATION OF THE PROPOSED METHOD**

**1. Angular partitioning**

Angular sections defined as  $\emptyset$  degree pieces on the  $\Omega$  image [19]. Number of pieces is k and the  $\emptyset = 2\pi/K$  equation is true (see Figure 3).According to Figure 3, if any rotation has been made on the image then pixels in section  $S_i$  will be moved to section  $S_j$  so that Equation 1 will be true.

$$j = (i + \lambda) \text{ mod } K, \text{ for } i, \lambda = 0, 1, 2, \dots, K - 1$$

feature of that slice. The scale and translation invariant image feature is then  $\{f(i)\}$  where

$$f(i) = \sum_{\theta = \frac{i2\pi}{K}}^{\frac{(i+1)2\pi}{K}} \sum_{\rho=0}^R \Omega(\rho, \theta) \text{ for } i = 0, 1, 2, \dots, K - 1$$

where  $R$  is the radius of the surrounding circle of the image.

When the considered image rotates to  $\tau = l2\pi/K$  radians ( $l = 0, 1, 2, \dots$ ) then its corresponding feature vector shifts circularly. To demonstrate this subject, let  $\Omega_\tau$  as counter counterclockwise rotated image of  $\Omega$  to  $\tau$  radians

$$\Omega_\tau(\rho, \theta) = \Omega(\rho, \theta - \tau)$$

So, the feature element of a considered.

In disc localization, the image  $I$  is divided into several concentric circles. The number of circles may be changed to get to best results. In disc localization, features are determined like angular partitioning, it means that I let the number of the edges pixels in each circle as a feature element. According to structure of this type of partitioning and because the centers of circles are one point, local information and feature values are not changed if a rotation

happened Therefore, we work on the gray image from green channel and the retinal blood vessels appear darker in the gray image.

Due to the acquisition process, retinal images often have a variation gray level contrast. In general, larger vessels display good contrast while the narrower ones show bad contrast. Thereby pixels attached to thick and thin vessels show the different gray level and geometrical correlation with the nearby pixels.

Normalization is performed to remove the gray-level deformation by subtracting [3] an approximate background from the original gray image. The approximate background is estimated using a  $75 \times 75$  median filter on the original retinal image. Thereby blood vessels are brighter than the background after Normalization.

The fuzzy C-means algorithm includes a multiplier field, which allows the centroids for each class to vary across the image. This helps us increase prominence of every finer detail of blood vessels irrespective of thick or thin. This generates the blood vessel segmentation even with thinnest one, which was irrecoverable until then.

#### IV. RESULTS AND DISCUSSION

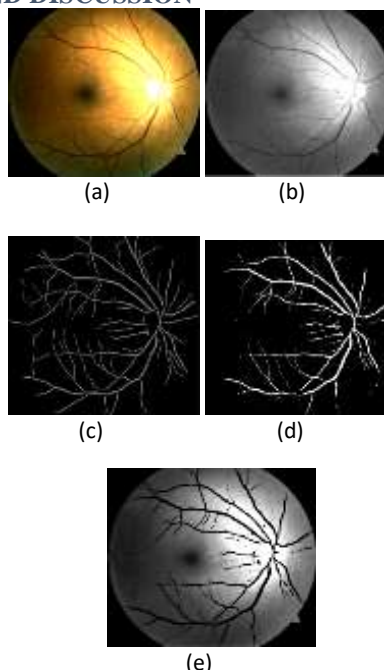


Figure 5. (a)Original image , (b)Gray scale image , (c) Hand drawn “ground truth” ,(d) Detected Blood Vessel using proposed method, (e) Blood vessel detected Image.

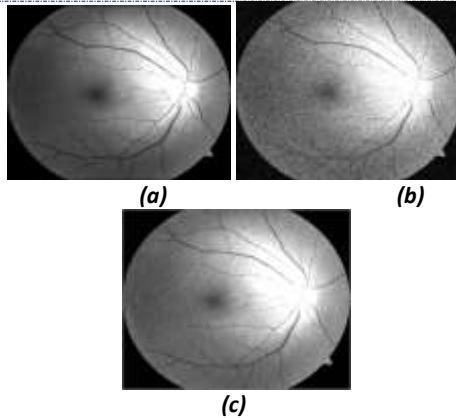


Figure 6. (a) Retinal Image (b) Stereoscopic Retinal Image (c) Denoised Image

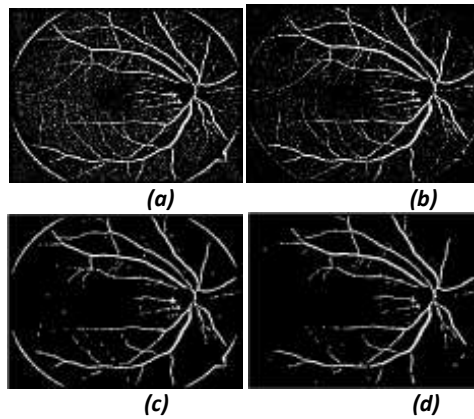


Figure 7. (a) FCM based segmented on stereoscopic Retinal Image (b) FCM based segmented image on denoised image (c) FCM based segmented on stereoscopic Retinal Image after filtering and removal small holes. (d) FCM based segmented on de-noised Retinal Image after filtering and removal small holes.

$$\begin{aligned}
 f_{\tau}(i) &= \sum_{\theta=\frac{K}{i}2\pi}^{\frac{(i+1)2\pi}{K}} \sum_{\rho=0}^R \Omega(\rho, \theta - \tau) \\
 &= \sum_{\theta=\frac{(i-1)2\pi}{K}}^{\frac{(i-1)2\pi}{K}} \sum_{\rho=0}^R \Omega(\rho, \theta) \\
 &= f(i-1)
 \end{aligned}$$

$$\text{Sensitivity (Ss)} = \frac{TP}{TP+FN}$$

$$\text{Specificity (Sp)} = \frac{TN}{TN+FP}$$

$$\text{PPV (Pv)} = \frac{TP}{TP+FP}$$

$$\text{PLR (Pr)} = \frac{TP/(TP+FN)}{FP/(FP+TN)}$$

$$\text{Accuracy (\%)} = \frac{TP + TN}{TP + TN + FP + FN}$$



Table 1.

Average Test Case:

Image	Sensitivity (Ss)	Specificity (SP)	PPV (PV)	PLR (PR)	Accuracy (%)
Retinal Image	99.62	54.66	95.08	219.72	95.03
Without Applying Bayes Soft Fundus detection on Stereoscopic Retinal Image	92.87	63.91	95.77	257.32	89.91
Only Applying Filter and removing small holes in the stereoscopic segmented image	98.29	51.82	94.72	203.99	93.54
After Applying Bayes Soft Fundus detection on Stereoscopic Retinal Image	96.51	0.6258	95.78	257.91	93.05
Applying Bayes Soft fundus detection on followed by filtering and removing small holes from the segmented retinal image	99.56	50.97	94.70	203.08	94.60

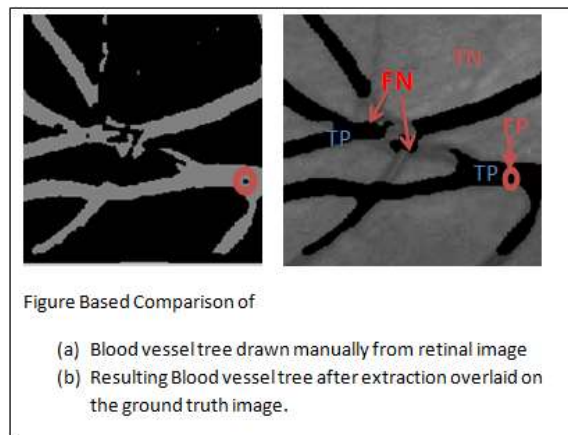


Figure 8. FN, TN, TP, FP

## V. CONCLUSION

In this present work, we deal with the hand drawn 'ground truth' and fuzzy segmented stereoscopic retinal blood vessel that appears split into two parts, i.e. thick and thin vessels according to the contrast. The input images for FCM based segmentation is not always be good quality in terms of sharpness, contrast, focus and etc for proper segmentation and often stereoscopic. Therefore, proper de-noising is required. The thick vessels are detected by adaptive local fundus detection in normalized images. The performance of the algorithm is measured against ophthalmologists' hand-drawn ground-truth. Sensitivity, specificity, PPV, PLR and sensitivity are used as the performance measurement of blood vessel detection because they combine true positive and false

positive rates. A comparative study shown in Fig. 3 denotes that very little part of the vessels was not segmented properly for this further optimization can be done. The efficacy of the present work demands to be more flawless compared to standard techniques as done by the physicians from their knowledge of experiences, the present work being result based using hand drawn “ground truth” image and the method claims the robustness against noise.

## VI. REFERENCES

1. Lili Xu, Shuqian Luo, “A novel method for blood vessel detection from retinal images”, Biomedical Engineering Online 2010, 9:14
2. Akara Sopharak, Bunyarit Uyyanonvara, Sarah Barman, “Automatic Exudate Detection from Non-dilated Diabetic Retinopathy Retinal Images Using Fuzzy C-means Clustering” Sensors 2009, 9, 2148-2161; doi:10.3390/s90302148
3. Ian NM, Patricia MH, R’John W: Image registration and subtraction for the visualization of change in diabetic retinopathy screening. Compute Med Imaging Graphics 2006, 30:139-145.]
4. Olson, J.A.; Strachana, F.M.; Hipwell, J.H. A comparative evaluation of digital imaging, retinal Photography and optometrist examination in screening for diabetic retinopathy. Diabet. Med. 2003, 20, 528-534. retinopathy screening. Compute Med Imaging Graphics 2006, 30:139-145.
5. George KM, Pantelis AA, Konstantinos KD, Nikolaos AM, Thierry GZ: Detection of glaucomatous change based on vessel shape analysis. Med Imaging Graphics 2006, 30:139-145.
6. T. Chanwimaluang and G. Fan. An efficient blood vessel detection algorithm for retinal images using local entropy fundus detection. In *Proc. of the IEEE Intl. Symp. on Circuits and Systems*, 2003.
7. Chih-Yin Ho1 and Tun-Wen Pai1, “An automatic fundus image analysis system for clinical diagnosis of glaucoma”, 2011 International Conference on Complex, Intelligent, and Software Intensive Systems
8. S. Chaudhuri, S. Chatterjee, N. Katz, M. Nelson, and M. Goldbaum. Detection of blood vessels in retinal images using two-dimensional matched filters. *IEEE Transactions on Medical Imaging*, 8(3):263269, 1989.
9. Giancardo, L.; Meriaudeau, F.; Karnowski, T. P.; Li, Y.; Garg, S.; Tobin, Jr, K. W.; Chaum, E. (2012), 'Exudate-based diabetic macular edema detection in fundus images using publicly available datasets.', *Medical Image Analysis* 16(1), 216--226.)
10. J. N. Ellinas, T. Mandadelis, A. Tzortzis, L. Aslanoglou, “Image de-noising using bartletts”, T.E.I. of Piraeus Applied Research Review, vol. IX, no. 1, pp. 97-109, 2004.
11. Azzopardi, G.; Petkov, N. Automatic detection of vascular bifurcations in segmented retinal images using trainable COSFIRE filters. *Pattern Recognition Lett.* **2013**, 34, 922–933.
12. Sabaghi, M.; Hadianamrei, S.R.; Zahedi, A.; Lahiji, M.N. A new partitioning method in frequency analysis of the retinal images for human identification. *J. Signal Inform. Process.* **2011**, 2, 274–278.
13. Barkhoda, W.; Tab, F.A.; Amiri, M.D. A Novel Rotation Invariant Retina Identification Based on the Sketch of Vessels Using Angular Partitioning. In *Proceedings of 4th International Symposium Advances in Artificial Intelligence and Applications*, Mragowo, Poland, 12–14 October 2009; pp. 3–6.
14. Amiri, M.D.; Tab, F.A.; Barkhoda, W. Retina Identification Based on the Pattern of Blood Vessels Using Angular and Disc localization. In *Advanced Concepts for Intelligent Vision Systems*; Springer: Berlin/Heidelberg, Germany, 2009; pp. 732–739.
15. Lowe, D.G. Object Recognition from Local Scale-Invariant Features. In *Proceedings of International Conference on Computer Vision*, Corfu, Greece, 20–27 September 1999; pp. 1150–1157.
16. Li, H.; Yang, H.; Shi, G.; Zhang, Y. Adaptive optics retinal image registration from scale-invariant feature transform. *Optik-Int. J. Light Electron Opt.* **2011**, 122, 839–841.
17. Li, H.; Lu, J.; Shi, G.; Zhang, Y. Tracking features in retinal images of adaptive optics confocal scanning laser ophthalmoscope using KLT-SIFT algorithm. *Biomed. Opt. Express* **2009**, 1, 31–40.
18. Marín, D.; Aquino, A.; Gegúndez-Arias, M.E.; Bravo, J.M. A new supervised method for blood vessel segmentation in retinal images by using gray-level and moment invariants-based features. *IEEE Trans. Med. Imaging* **2011**, 30, 146–158.

## CITE AN ARTICLE

Pal, M., Ray, R., & Choudhury, N. (n.d.). FUZZY LOGIC BASED OPTICAL DISC LOCALIZATION AND DETECTION OF STEREOSCOPIC RETINAL IMAGES IN NROI. *INTERNATIONAL JOURNAL OF ENGINEERING SCIENCES & RESEARCH TECHNOLOGY*, 6(12), 84-93.